Snelling, EP, Seymour, RS, Giussani, DA, Fuller, A, Maloney, SK, Farrell, AP, Mitchell, D, George, KP, Dzialowski, EM, Jonker, SS and Wube, T

Scaling of cardiac morphology is interrupted by birth in the developing sheep Ovis aries.

Scaling of cardiac morphology is interrupted by birth in the developing sheep *Ovis aries*

Edward P Snelling [1], Roger S Seymour [2], Dino A Giussani [3], Andrea Fuller [1], Shane K Maloney [1,4], Anthony P Farrell [5,6], Duncan Mitchell [1,4], Keith P. George [7], Edward M. Dzialowski [8], Sonnet S. Jonker [9], Tilaye Wube [10]

[1] Brain Function Research Group, School of Physiology, University of the Witwatersrand, Johannesburg, Gauteng, South Africa; [2] School of Biological Sciences, University of Adelaide, Adelaide, South Australia, Australia; [3] Department of Physiology, Development and Neuroscience, University of Cambridge, Cambridge, United Kingdom; [4] School of Human Sciences, University of Western Australia, Crawley, Western Australia, Australia; [5] Department of Zoology, University of British Columbia, Vancouver, British Columbia, Canada; [6] Faculty of Land and Food Systems, University of British Columbia, Vancouver, British Columbia, Canada; [7] Research Institute for Sport and Exercise Sciences, Liverpool John Moores University, Liverpool, United Kingdom; [8] Developmental Integrative Biology Research Group, Department of Biological Sciences, University of North Texas, Denton, Texas, United States; [9] Knight Cardiovascular Institute, Oregon Health and Science University, Portland, Oregon, United States; [10] Department of Zoological Sciences, Addis Ababa University, Addis Ababa, Ethiopia

Running head: Scaling of cardiac morphology in sheep

Author for correspondence:
Edward P Snelling,
Brain Function Research Group, School of Physiology,
7 York Road, Parktown Medical Campus,
University of the Witwatersrand, Johannesburg, South Africa 2193.
Phone: +27 11 717 2152, Facsimile: +27 11 643 2765, Email: edward.snelling@wits.ac.za

Abstract

Scaling of the heart across development can reveal the degree to which variation in cardiac morphology depends on body mass. In this study, we assessed the scaling of heart mass, left and right ventricular masses, and ventricular mass ratio, as a function of eviscerated body mass across fetal and postnatal development in Horro sheep *Ovis aries* (~50-fold body mass range; $N = 21$). Whole hearts were extracted from carcasses, cleaned, dissected into chambers, and weighed. We found a biphasic relationship when heart mass was scaled against body mass, with a conspicuous 'breakpoint' around the time of birth, manifest not by a change in the scaling exponent (slope), but rather a jump in the elevation. Fetal heart mass (g) increased with eviscerated body mass (M_b, kg) according to the power equation $4.90M_b^{0.88 \pm 0.26 (\pm 95\% CI)}$, whereas postnatal heart mass increased according to $10.0M_b^{0.88 \pm 0.10}$. While the fetal and postnatal scaling exponents are identical (0.88) and reveal a clear dependence of heart mass on body mass, only the postnatal exponent is significantly less than 1.0, indicating the postnatal heart becomes a smaller component of body mass as the body grows, which is a pattern found frequently with postnatal cardiac development among mammals. The rapid doubling in heart mass around the time of birth is independent of any increase in body mass and consistent with the normalization of wall stress in response to abrupt changes in volume loading and pressure loading at parturition. We discuss variation in scaling patterns of heart mass across development among mammals, and suggest that the variation results from a complex interplay between hard-wired genetics and epigenetic influences.

Key words: allometry, biphasic, cardiac, fetal, morphogenesis, ontogeny

Introduction

Cardiogenesis, growth and remodeling of the heart are driven by an orchestrated program of gene activation and repression under the precise spatial and temporal control of transcription factors and microRNAs (Roche et al., 2013; Sylva et al., 2014). Biomechanical forces exerted by blood on the walls of the heart shape the phenotype by inducing gene expression and differentiation necessary for normal developmental patterning (Lindsey et al., 2014). The embryonic heart forms when cardiac progenitor cells arise from the mesoderm and establish in the cranial region of the embryo, where they arrange to form the cardiac crescent, before coalescing and fusing into a single cardiac tube that undergoes looping and 'ballooning' of the chambers (Christoffels et al., 2000; Moorman & Christoffels, 2003). The fetal heart takes form when the chambers and outflow tract undergo septation, a compact myocardium is laid down, and leaflet valves develop (Fig 1a). The fetal heart nonetheless maintains a small fissure through the atrial septum, the *foramen ovale*, which allows for right-to-left atrial shunting, while the thicker ventricular septum completely separates the left and right ventricles (Sylva et al., 2014). A compact myocardium forms at the epicardial side of the developing fetal heart (Ieda et al., 2009), and soon after the newly formed coronary vascular network connects with the base of the aorta, becoming functional, and allows perfusion of the compact cardiac tissue (Tomanek, 1996; Farrell, 1997; Farrell et al., 2012). Facilitated by an increasing role of the sinoatrial and atrioventricular nodes in the fetal heart, a mature apex-to-base activation sequence of the septated ventricles arises (Sedmera & Ošťádal, 2012). Leaflet valves form at the atrioventricular canals, and at the aortic and pulmonary outflow tracts, ensuring the unidirectional flow of fetal blood (Sedmera & Ošťádal, 2012). Across gestation, the fetal heart increases in absolute mass, and increases its capacity to generate both absolute blood flow (Rudolph & Heymann, 1970) and blood pressure (Dawes et al., 1980; Kitanaka et al., 1989; Giussani et al., 2005).

At birth, the transition from placental to pulmonary gas exchange changes significantly the flow and pressure requirements of the heart. The placental circulation is eliminated, and there is closure of the *foramen ovale* between the atrial chambers, closure of the *ductus arteriosus* channel between pulmonary artery and aorta, and closure of the *ductus venosus* channel that bypasses the liver (Rudolph, 1970;

Thornburg et al., 1997). With this re-plumbing, the left and right ventricular chambers adjust from working against the same blood pressure with different blood flow outputs *in utero* to working against significantly different blood pressures but with identical blood flow outputs *post utero*. The postnatal heart also has to deal for the first time with the effects of gravity. Measurements from sheep, taken before and soon after birth, document an increase in the mass-specific cardiac outputs of both ventricular chambers, with the left ventricle in particular increasing from ca. 150 to 300 – 450 mL min^{-1} kg^{-1} over this brief perinatal period (original data or summarised in Klopfenstein & Rudolph, 1978; Lister et al., 1979; Anderson et al., 1981; Heymann et al., 1981; Rudolph, 1985; Morton et al., 1987; Stopfkuchen, 1987; Grant, 1999). The increase in left ventricular cardiac output is achieved in large part by an increase in the mass-specific stroke volume, which doubles, from ca. 1 to 2 mL kg^{-1}. The large increase in left ventricular mass-specific stroke volume at birth is congruent with reports that heart growth after birth is disproportionately in favour of the left ventricle over the right ventricle (Lee et al., 1975), a process thought to involve accelerated proliferation and enlargement of the left ventricular cardiomyocytes (Smolich et al., 1989). As the postnatal heart continues to grow and mature to adulthood, there is an associated rise in absolute cardiac output (Woods Jr et al., 1978), although the increase in systemic arterial blood pressure is comparatively minor (Berman & Christensen, 1983).

Despite recent advancements to our qualitative understanding of cardiac development (Roche et al., 2013; Sylva et al., 2014), our quantitative understanding has not kept pace, in part because of our failure to account for the non-linear effects of body size on cardiac structure and function (Calder III, 1996; Batterham et al., 1999; Chantler et al., 2005). One way of describing cardiac structure and function is by scaling analysis (allometry), which relates an anatomical or physiological cardiac variable (Y) to body mass (M_b), usually by a power equation, $Y = aM_b^{\,b}$, where a (the coefficient) represents the elevation of the curvilinear line (value of Y when $M_b = 1$), and b (the exponent) describes the shape of the curvilinear line (Fig 1b). If b = 1, then Y increases in direct proportion to M_b; if b = 0, Y is independent of M_b; if 1 > b > 0, Y increases with a curve that has a decreasing slope against M_b; if b > 1, Y increases with a curve with an increasing slope against M_b; and if 0 > b > –1, Y decreases with a curve that has a decreasing

slope against M_b. Logarithmic transformation of the data straightens the line for statistical interrogation, and the rearranged equation becomes, $\log Y = \log a + b \log M_b$, where loga now represents the elevation of the linearized relationship (y-intercept, value of log$Y$ when $\log M_b = 0$), and b is unchanged but now defines the slope of the linearized relationship. Thus, in reference to b, the terms 'slope' and 'exponent' are often used interchangeably.

Previous scaling analyses on a variety of mammal species reveal that heart mass increases with body mass across postnatal development according to a power equation with a scaling exponent (slope) that usually is less than 1.0, meaning that the ratio of heart mass to body mass decreases as the body grows across postnatal life (summarised in Snelling et al., 2015a). This supports earlier observations that the neonate heart is relatively larger than the adult heart in several species of laboratory and domestic mammals (Lee et al., 1975). Scaling studies that have broadened the analysis to include the fetal life stage of placental mammals and the in-pouch life stage of marsupial mammals have led to the suggestion that heart mass has a biphasic relationship with body mass, with a 'breakpoint' at which the exponent (slope) changes at birth and at pouch exit in these respective groups. In humans, the heart mass exponent is reported to be 1.19 across fetal development and 0.89 across postnatal development (Hirokawa, 1972), which implies that before birth, but not after birth, cardiac growth outpaces that of body mass. However, that study obtained its data from spontaneously aborted fetuses, many with known cardiopulmonary disease. In giraffes *Giraffa camelopardalis*, the fetal heart mass exponent is 1.03 and the postnatal exponent is 0.90 (Mitchell & Skinner, 2009). However, adult giraffes are unusual in that their long vertical heart-to-head distance requires them to generate exceptionally high mean central arterial blood pressures, achieved by a relatively thick-walled left ventricle (Smerup et al., 2016), but it is unclear when those high blood pressures first appear during development. Two studies give different patterns of cardiac growth in two different species of marsupial, which give birth to extremely altricial, ectothermic-young that develop within a pouch. For the western grey kangaroo *Macropus fuliginosus*, the in-pouch heart mass exponent is 1.10 and the post-pouch exponent is 0.77 (Snelling et al., 2015a). However, in the tammar wallaby *Macropus eugenii*, heart mass scales in perfect isometry with body mass (exponent of

125 1.0) across the full scope of development with no detectable breakpoint between in-pouch and post-pouch
126 life stages (Hulbert et al., 1991). Thus, there is reason to question the generality of a biphasic scaling
127 pattern of heart mass growth across development in mammals.
128 In this study, we assessed the scaling of cardiac morphology across fetal and postnatal development
129 in Horro sheep *Ovis aries*, a common breed of Ethiopia readily available to us. Using this sheep as a
130 model, we seek further evidence for or against a biphasic scaling pattern of heart mass across
131 development, and we investigate if the apparent doubling of left ventricular mass-specific stroke volume
132 at birth is reflected in the gross morphology of the heart. Scaling relationships are presented for whole
133 heart mass, left ventricular (LV) mass, right ventricular (RV) mass, and ventricular mass ratio (RV/LV).

Materials and methods

Animal carcasses

This study was approved by the Animal Ethics Committees of the University of the Witwatersrand (2017/05/33/0) and Addis Ababa University (427/09/2017). In cooperation with local abattoirs in Addis Ababa, we purchased whole hearts extracted from carcasses of Horro sheep *Ovis aries*, a short-fleeced, medium-sized breed from Ethiopia, with nothing unusual in its morphology (Gizaw et al., 2008). The Horro sheep were supplied by nearby farms, from a mid-altitude region, approximately 2500 m above sea level. Typically, the Horro sheep has a birth body mass of 2.7 kg, a weaning body mass of 12 kg (ca. 93 days), a mature body mass of 25 – 35 kg, and an average litter size of 1.34 (Abegaz et al., 2000; Ermias et al., 2006). The abattoir workers killed each postnatal sheep according to their standard practice, before eviscerating the carcass, removing the gastrointestinal tract and its contents, but leaving behind all other internal organs. Eviscerated body mass was recorded to the nearest 0.01 kg on a calibrated digital strain gauge scale (PK-110; AWS, Cumming, GA, USA). The abattoir workers then removed the hearts, and we sealed them in plastic zip-lock bags, transported them back to the laboratory, and froze them until day of dissection. In addition, the abattoirs supplied us with fetal carcasses. For consistency, we sealed and transported these fetal carcasses in plastic zip-lock bags and froze them until day of dissection, at which time we weighed them, removed the gastrointestinal tract, and reweighed them, and then removed the heart for dissection. We recorded their intact total body mass and their eviscerated body mass to the same precision using the same strain gauge scale as for the postnatal sheep.

Heart dissections

We obtained 30 hearts from sheep carcasses, from which we measured 10 fetal hearts and 11 postnatal hearts. We excluded 9 hearts that were either not fully formed (e.g., incomplete septation) or not extracted whole by the abattoir workers (e.g., missing atrial chamber). We emptied the chambers of congealed blood, removed major blood vessels, trimmed any excess fat, and dissected the chambers from one another. For both fetal and postnatal hearts, we excised the LV free wall plus the interventricular

160 septum ('left ventricle'), and the RV free wall ('right ventricle'), following what have become standard
161 procedures (Fulton et al., 1952; Keen, 1955; Joyce et al., 2004; Snelling et al., 2016). The myocardial
162 mass of each chamber was determined by weighing to the nearest 0.01 g on a calibrated analytical balance
163 (ADP-2100; Adam Equipment, Milton Keynes, UK) and the chamber masses summed to provide whole
164 heart mass.
165
166 *Statistical analyses*
167 Scaling relationships are presented to describe the change in whole heart mass (atria + ventricles), LV
168 mass, RV mass, and ventricular mass ratio (RV/LV), each as a function of eviscerated body mass, across
169 fetal and postnatal development in Horro sheep. The scaling relationships are in the form of a power
170 equation, $Y = aM_b^{\,b \pm 95\%\ CI}$, where Y is the cardiac variable of interest, a is the scaling coefficient
171 (elevation), b is the scaling exponent (slope of the log-transformed relationship), M_b is the eviscerated
172 body mass in kg, and CI stands for confidence interval. To analyse the scaling relationships statistically,
173 we took the $\log_{10}$ of the cardiac variable and the $\log_{10}$ of eviscerated body mass, and applied ordinary
174 least-squares linear regressions to the log-transformed data (Smith, 2009; Kilmer & Rodriguez, 2017). To
175 determine whether heart mass had a biphasic relationship with body mass, we performed a broken stick
176 analysis by fitting a series of two-phase linear regressions to the log-transformed data. We identified the
177 breakpoint as the intersection that minimised the sum for both 'sticks' of the regressions' residual sums of
178 squares (Yeager & Ultsch, 1989; Mueller & Seymour, 2011). The slopes and elevations of the
179 regressions then were compared between fetal and postnatal life stages by ANCOVA (Zar, 1998) by
180 means of dedicated statistical software (Prism 7; GraphPad Software, La Jolla, CA, USA).

181 Results

182 *Scaling of whole heart mass*

183 When the fetal and postnatal life stages of Horro sheep are combined, whole heart mass increases with
184 eviscerated body mass according to a power equation with a scaling exponent of 1.12 ± 0.11 (± 95% CI)
185 (Fig 2a). However, this analysis obscures a clear biphasic relationship, driven by a doubling in whole
186 heart mass around the time of birth (Fig 2b). The increase appears to be real, not a statistical artefact, and
187 is confirmed by the broken stick analysis, which identified the breakpoint at birth. When considered
188 separately, the fetal and postnatal life stages have the same scaling exponent for heart mass against
189 eviscerated body mass (0.88 ± 0.26 and 0.88 ± 0.10, respectively; ANCOVA, $P = 0.96$), but the scaling
190 elevations are markedly and statistically different ($P < 0.0001$; Table 1). While the identical exponent
191 (0.88) seems to imply that neither fetal nor postnatal cardiac growth keeps pace with body mass, the fetal
192 heart mass exponent is not significantly different from isometry (95% CI overlaps 1.0), and only the
193 postnatal exponent shows statistical hypoallometry (95% CI less than 1.0).

194

195 *Scaling of LV and RV masses*

196 The scaling exponents for LV mass against eviscerated body mass are statistically indistinguishable
197 across fetal and postnatal development, 0.90 ± 0.35 and 0.90 ± 0.11, respectively (ANCOVA, $P = 0.99$),
198 but the scaling elevations are significantly different ($P < 0.0001$; Fig 3a). Likewise, the exponents for RV
199 mass against eviscerated body mass are statistically indistinguishable across fetal and postnatal
200 development, 0.93 ± 0.23 and 0.92 ± 0.13, respectively ($P = 0.87$), but in this case of the RV, the
201 elevations are not statistically different ($P = 0.07$; Fig 3b). Therefore, the 2.0-fold increase in whole heart
202 mass around the time of birth is due to an increase in LV mass (2.4-fold) rather than RV mass (1.3-fold).
203 Indeed, the ventricular mass ratio (RV/LV) changes around the time of birth (Fig 3c), from an average
204 ratio of 0.60 ± 0.10 across fetal development (exponent of 0.04 ± 0.30) to an average ratio of 0.33 ± 0.03
205 across postnatal development (exponent of 0.02 ± 0.15).

206 Discussion

207 This study used scaling analysis to track change in cardiac morphology, as a function of eviscerated body
208 mass, across fetal and postnatal development in Horro sheep. Previous scaling studies of humans
209 (Hirokawa, 1972), giraffes (Mitchell & Skinner, 2009), and kangaroos (Snelling et al., 2015a) revealed a
210 biphasic relationship between heart mass and body mass, with heart mass increasing with a relatively
211 steep exponent (slope) across fetal or in-pouch life, before transitioning to a shallower exponent across
212 postnatal or post-pouch life. However, that pattern was not apparent in Horro sheep. Instead, the scaling
213 exponents for heart mass are identical before and after parturition, and the breakpoint around the time of
214 birth is manifest as a jump in the elevation. The resetting of elevation is almost entirely due to a rapid
215 increase in LV mass during the perinatal period. We begin this discussion by assessing the likely effect
216 of using eviscerated body mass, rather than intact total body mass, as the independent variable in the
217 scaling analysis. Next, we show how the rapid increase in heart mass around the time of birth is
218 consistent with well-documented changes in mass-specific stroke volumes and arterial blood pressures
219 recorded from near-term fetal sheep and 1-week-old neonatal lambs. Lastly, we discuss the implications
220 of heart mass scaling across fetal and postnatal development and its relationship to whole body
221 physiology.

222

223 *Effect of using eviscerated body mass in the scaling analysis*

224 Our postnatal Horro sheep were sourced as fresh, eviscerated carcasses from abattoirs and, as such, our
225 eviscerated body mass omits the masses of the gastrointestinal tract, its foodstuff contents, and some
226 blood. A previous study on the postnatal Horro sheep indicates that eviscerated body mass is
227 approximately 25% lower than intact total body mass (Ermias et al., 2006), although it is unclear if this
228 proportion changes with postnatal body growth. Our fetal sheep were weighed before and after
229 evisceration, with eviscerated body mass 8% lower than intact total body mass, and the deficit
230 independent of fetal body growth. If, instead, we use fetal total body masses and if we apply a +25%
231 adjustment to our postnatal eviscerated body masses, the exponent describing heart mass as a function of

body mass across fetal and postnatal life stages combined decreases from 1.12 ± 0.11 to 1.05 ± 0.08 (Fig 2a). However, the adjustment does not affect the scaling exponents of the fetal and postnatal life stages when they are treated separately, but the magnitude of the jump in heart mass around the time of birth is reduced from 2.0-fold to 1.7-fold (Fig 2b). Thus, our observation concerning the different fetal and postnatal scaling elevations is not an artefact resulting from the use of eviscerated body mass rather than total body mass.

Scaling of cardiac morphology is interrupted by birth

At birth, the precocial neonate for the first time must satisfy the energy-intensive tasks of endothermy, independent locomotion, and independent nutrition. The heart and circulation remodel from parallel circuits incorporating the placenta to an in-series circuit via the lungs. Associated with this remodeling, the left and right ventricular chambers transition from working against the same blood pressure with different blood flow outputs *in utero* to working against significantly different blood pressures but with identical blood flow outputs *post utero* (Rudolph, 1970; Thornburg et al., 1997). It is congruent then that our scaling analysis reveals a biphasic relationship between heart mass and body mass in Horro sheep, with a breakpoint occurring around the time of birth, in the form of a 2.0-fold increase in heart mass, driven primarily by a 2.4-fold increase in LV mass (Fig 3a), and supplemented by a not-statistically-significant 1.3-fold increase in RV mass (Fig 3b). Evidence for the capacity of the perinatal heart to rapidly gain myocardial mass, independent of any increase body mass, comes primarily from studies of near-term fetal sheep, where experimentally-increased RV wall stress levels, induced by partial occlusion of the pulmonary artery, elicit a 1.3 to 1.7-fold increase in mass-specific heart mass within 7 – 10 days (Barbera et al., 2000; Segar et al., 2013). The rapid increase in LV mass around the time of birth in our Horro sheep also aligns with two previous reports of a sharp ~1.3-fold increase in LV end-diastolic and end-systolic linear dimensions in near-term fetal sheep compared to 2-day-old neonatal lambs (Kirkpatrick et al., 1973; Anderson et al., 1984). Although the two studies did not consider the effects of body size, a 1.3-fold increase in linear dimensions of the heart, raised to the third power, equates to a 2.2-

fold increase in volumetric dimensions of the heart, which we assume greatly exceeds the increase in body size over the first two days of postnatal life. It has been suggested that at birth, the removal of constraints that are caused by tissues surrounding the heart (e.g., fluid-filled lungs) allows for a near-immediate increase in LV end-diastolic dimensions and preload, and thus facilitates increased LV stroke volume in the neonate (Grant, 1999; Grant et al., 2001).

The biphasic scaling pattern of heart mass across development in Horro sheep, characterized by a rapid increase in heart mass around the time of birth, and independent of any increase in body mass, is not without precedent. Indeed, a recent scaling study showed a conspicuous breakpoint effected by a rapid 1.6-fold increase in the elevation of heart mass at hatching, in another precocial endotherm with a four-chambered heart, the Pekin duck *Anas platyrhynchos domestica* (Fig 4a; Sirsat et al., 2016). Nonetheless, the breakpoint in the scaling elevation of Horro sheep differs from what we found when we reanalyzed published heart mass and body mass data for sheep of mixed Western breeds. That analysis revealed a breakpoint in the scaling exponent rather than elevation around the time of birth, with a relatively steep gain in heart mass across fetal development transitioning to a hypoallometric trajectory across postnatal development (Fig 4b; Jonker et al., 2015). Likewise, two previous studies on placental mammals (humans and giraffes) reported a breakpoint in the scaling exponent around the time of birth (Hirokawa, 1972; Mitchell & Skinner, 2009). These differences among studies warrant future work because the substantial widening of the ventricular mass ratio (RV/LV) around the perinatal period [from 0.60 in the fetal heart to 0.33 in the postnatal heart, as a result of the disproportionate increase in LV mass compared to RV mass] has been reported widely for other placental mammals (Lee et al., 1975). In humans, the ratio decreases from 0.8 at birth, to 0.6 within a few days after birth, and to 0.4 by 3 months of age (Keen, 1955; Joyce et al., 2004).

The rapid increase in LV mass, but not RV mass, that we observed in Horro sheep is consistent with the different changes in volume loading and pressure loading on the chambers at birth. In accordance with the Principle of Laplace, an approximate model for mean circumferential wall stress (σ) of a thick-walled sphere is given by the relationship, $\sigma = r_i P_t / 2h$, where r_i is internal radius, P_t is

transmural pressure and h is wall thickness (Mirsky, 1974; Westerhof et al., 2010). Although the chambers of the heart are not exactly thick-walled spheres, and although their geometry likely changes with remodeling at birth, this formula nonetheless shows that, if other variables are held constant, an increase in either volume loading ($\uparrow r_i$) or pressure loading ($\uparrow P_t$) on the chamber walls, would require an increase in wall thickness ($\uparrow h$) to spread the additional load and normalize mean circumferential wall stress (Seymour & Blaylock, 2000). Therefore, we posit that the 2.4-fold increase in LV mass at around the time of birth, which occurs independent of changes in body mass, likely reflects an increase in LV wall thickness to normalize wall stress in response to an abrupt increase in volume loading (i.e., end-diastolic volume). The evidence for the increase in volume loading comes from studies that report an increase in mass-specific LV stroke volume around the time of birth (assuming constant ejection fraction), which doubles from approximately 1 mL kg^{-1} in near-term fetal sheep to 2 mL kg^{-1} in 1-week-old neonatal lambs (original data or summarised in Klopfenstein & Rudolph, 1978; Lister et al., 1979; Anderson et al., 1981; Morton et al., 1987; Stopfkuchen, 1987; Grant, 1999). Indeed, a comparable increase in LV mass-specific stroke volume has been recorded from near-term fetal sheep subject to artificial positive pressure ventilation simulating birth (Teitel et al., 1987). To a slightly lesser extent, the increase in LV mass around the time of birth also is likely a consequence of an increase in LV wall thickness due to an increase in pressure loading. The evidence for the increase in pressure loading comes from studies that report an increase in left-sided blood pressure from approximately 50 mmHg in near-term fetal sheep to 70 mmHg in newborn lambs (summarised in Grant, 1999; Jonker & Louey, 2016). Once again in accordance with the Principle of Laplace, we posit that the lack of a significant increase in RV mass around the time of birth likely results from the absence of a substantial change in RV wall thickness, at least partly due to the counteracting effects of an increase in volume loading and a decrease in pressure loading. On the one hand, RV volume loading likely increases around the time of birth based on studies that report a ~1.2-fold increase in mass-specific RV stroke volume (assuming constant ejection fraction), from approximately 1.7 mL kg^{-1} in near-term fetal sheep to 2 mL kg^{-1} in 1-week-old neonatal lambs (original data or summarised in Klopfenstein & Rudolph, 1978; Lister et al., 1979; Anderson et al.,

1981; Morton et al., 1987). On the other hand, and probably of greater importance, RV pressure loading likely decreases around the time of birth due to an abrupt decrease in right-sided blood pressure, which drops from approximately 50 mmHg in near-term fetal sheep to 20 – 30 mmHg in newborn lambs (summarised in Grant, 1999; Jonker & Louey, 2016). While we have left aside the important influence of the geometry of the ventricular chambers, it is worth noting that the postnatal RV remains relatively thick walled, given the low pressure it generates compared to the postnatal LV, probably as a consequence of its larger radius of curvature, which places the RV at a disadvantage in the development of pressure (Huisman et al., 1980).

Scaling of cardiac morphology across fetal and postnatal life

The properties of the scaling of heart mass across fetal and postnatal development have other physiological implications. In Horro sheep, fetal heart mass scales against body mass with a somewhat shallow exponent of 0.88, not quite statistically different from 1.0 in our modest sample. However, across fetal development, the maturation of cardiomyocyte ultrastructure will have implications for cardiac function. Studies on the hearts of sheep and other placental mammals collectively show that across fetal development (and sometimes extending into the neonatal period), there is a general improvement in the alignment and organization of the myofilaments and myofibrils, and often a notable increase in the volume densities of the myofibrils and mitochondria (Canale et al., 1986). Those changes are concomitant with an increased contractile performance of isolated strips of myocardium and likely contribute to the augmented functional performance of the whole heart (Canale et al., 1986; Smolich, 1995; Anderson, 1996). Indeed, a previous scaling analysis has shown maturation of cardiomyocyte ultrastructure occurring during in-pouch development of the marsupial western grey kangaroo (Snelling et al., 2015b). Myofibril and mitochondrial volume densities increase with respective scaling exponents of 0.13 ± 0.06 and 0.04 ± 0.03, likely facilitating an increase in the functional performance of the heart as the growing in-pouch young develop endothermy and become independently mobile. If a similar maturation of cardiomyocyte ultrastructure and function occurs during fetal development of the Horro

sheep, then it will provide some compensation for the shallow scaling of fetal heart mass. To date, no study has examined the scaling of cardiac ultrastructure, nor its relationship to cardiac performance and whole body metabolic requirements, across the fetal and postnatal development of any placental mammal.

The hypoallometry of heart mass against body mass across the postnatal and post-pouch development of mammals is common, although the range of scaling exponents is surprisingly broad, typically from 0.7 to 1.0 (summarised in Snelling et al., 2015a). The present study with Horro sheep revealed a postnatal exponent of 0.88, a value that is significantly lower than 1.0. An even shallower exponent of 0.78 from sheep of mixed Western breeds implies that a more severe hypoallometry of postnatal heart mass is possible (Jonker et al., 2015). In the marsupial western grey kangaroo, heart mass scales with a hypoallometric exponent of 0.77 across post-pouch development (Snelling et al., 2015a) despite the cardiomyocytes attaining ultrastructural maturity at pouch exit (Snelling et al., 2015b). The reason why the growing heart tends to become relatively smaller as body mass increases across postnatal development is probably varied and complex. Nevertheless, these comparisons seem to reinforce our overall finding that there is much variation in the scaling patterns of heart mass against body mass across development among mammals. The diversity of the observed scaling patterns likely arises from the complex interplay between hard-wired genetic growth and maturation of the heart, and the influence of epigenetic factors on the phenotype of the heart. Because of this interplay, we cannot yet generalize on the exact scaling of either form or function of the heart across development, or the rationale behind the scaling.

Conclusions

In this study, we use Horro sheep to demonstrate the utility of scaling in teasing apart changes in cardiac morphology that are related to changes in body mass, and those that occur independently of body mass, at different stages of development. We found that heart mass scales against eviscerated body mass with an identical exponent of 0.88 over both the fetal and the postnatal life stages, but that the scaling elevations differ significantly due to a rapid doubling in heart mass around the time of birth. This increase in heart

362 mass occurs independent of any change in body mass, and appears congruent with the normalization of
363 wall stress in response to changing volume loading and pressure loading on the ventricular walls at
364 parturition. We also show that the pattern of scaling of heart mass against body mass across development
365 among mammals varies greatly, likely resulting from a complex interplay between hard-wired genetics
366 and epigenetic influences.

Acknowledgments

The authors acknowledge the College of Natural Sciences, Addis Ababa University, for providing support and facilities. We also thank Anteneh Tesfaye for assistance with the dissections. This research was supported by Company of Biologists, Journal of Experimental Biology, and Society for Experimental Biology awards to EPS and TW, a University of the Witwatersrand FRC Individual Grant and Iris Ellen Hodges Fund awards to EPS and AF, and a South African Claude Leon Foundation Postdoctoral Fellowship to EPS. APF holds a Canada Research Chair.

Author contributions

All authors contributed significantly to the study.

Conflict of interest

No conflicts of interest, financial or otherwise, are declared by the authors.

References

Abegaz S, Gemeda D, Rege JEO, et al. (2000) Early growth, survival and litter size in Ethiopian Horro sheep. *S Afr J Anim Sci* **30 (Supplement 1),** 1-3.

Anderson DF, Bissonnette JM, Faber JJ, et al. (1981) Central shunt flows and pressures in the mature fetal lamb. *Am J Physiol* **241,** H60-H66.

Anderson PAW (1996) The heart and development. *Semin Perinatol* **20,** 482-509.

Anderson PAW, Glick KL, Manring A, et al. (1984) Developmental changes in cardiac contractility in fetal and postnatal sheep: *in vitro* and *in vivo*. *Am J Physiol* **247,** H371-H379.

Barbera A, Giraud GD, Reller MD, et al. (2000) Right ventricular systolic pressure load alters myocyte maturation in fetal sheep. *Am J Physiol* **279,** R1157-R1164.

Batterham AM, George KP, Whyte G, et al. (1999) Scaling cardiac structural data by body dimensions: a review of theory, practice, and problems. *Int J Sports Med* **20,** 495-502.

Berman W, Christensen D (1983) Effects of acute preload and afterload stress on myocardial function in newborn and adult sheep. *Biol Neonate* **43,** 61-66.

Calder III WA (1996) *Size, Function, and Life History,* Dover Publications, New York.

Canale ED, Campbell GR, Smolich JJ, et al. (1986) *Cardiac Muscle, pp 165-171,* Springer-Verlag, Berlin.

Chantler PD, Clements RE, Sharp L, et al. (2005) The influence of body size on measurements of overall cardiac function. *Am J Physiol* **289,** H2059-H2065.

Christoffels VM, Habets PEMH, Franco D, et al. (2000) Chamber formation and morphogenesis in the developing mammalian heart. *Dev Biol* **223,** 266-278.

Dawes GS, Johnston BM, Walker DW (1980) Relationship of arterial pressure and heart rate in fetal, new-born and adult sheep. *J Physiol (London)* **309,** 405-417.

Ermias E, Yami A, Rege JEO (2006) Slaughter characteristics of Menz and Horro sheep. *Small Ruminant Res* **64,** 10-15.

Farrell AP (1997) Evolution of cardiovascular systems: insights into ontogeny. In *Development of Cardiovascular Systems: Molecules to Organisms* (eds Burggren WW, Keller BB), pp. 101-113. Cambridge: Cambridge University Press.

Farrell AP, Farrell ND, Jourdan H, et al. (2012) A perspective on the evolution of the coronary circulation in fishes and the transition to terrestrial life. In *Ontogeny and Phylogeny of the Vertebrate Heart* (eds Sedmera D, Wang T), pp. 75-102. New York: Springer.

Fulton RM, Hutchinson EC, Jones AM (1952) Ventricular weight in cardiac hypertrophy. *Br Heart J* **14,** 413-420.

Giussani DA, Forhead AJ, Fowden AL (2005) Development of cardiovascular function in the horse fetus. *J Physiol (London)* **565,** 1019-1030.

Gizaw S, Komen H, Hanotte O, et al. (2008) Indigenous sheep resources of Ethiopia: types, production systems and farmers preferences. *AGRI* **43,** 25-39.

Grant DA (1999) Ventricular constraint in the fetus and newborn. *Can J Cardiol* **15,** 95-104.

Grant DA, Fauchère JC, Eede KJ, et al. (2001) Left ventricular stroke volume in the fetal sheep is limited by extracardiac constraint and arterial pressure. *J Physiol (London)* **535,** 231-239.

Heymann MA, Iwamoto HS, Rudolph AM (1981) Factors affecting changes in the neonatal systemic circulation. *Annu Rev Physiol* **43,** 371-383.

Hirokawa K (1972) A quantitative study on pre- and postnatal growth of human heart. *Acta Pathol Jpn* **22,** 613-624.

Huisman RM, Sipkema P, Westerhof N, et al. (1980) Comparison of models used to calculate left ventricular wall force. *Med Biol Eng Comput* **18,** 133-144.

Hulbert AJ, Mantaj W, Janssens PA (1991) Development of mammalian endothermic metabolism: quantitative changes in tissue mitochondria. *Am J Physiol* **261,** R561-R568.

Ieda M, Tsuchihashi T, Ivey KN, et al. (2009) Cardiac fibroblasts regulate myocardial proliferation through β1 integrin signaling. *Dev Cell* **16,** 233-244.

Jonker SS, Louey S (2016) Endocrine and other physiologic modulators of perinatal cardiomyocyte endowment. *J Endocrinol* **228,** R1-R18.
Jonker SS, Louey S, Giraud GD, et al. (2015) Timing of cardiomyocyte growth, maturation, and attrition in perinatal sheep. *FASEB J* **29,** 4346-4357.
Joyce JJ, Dickson PI, Qi N, et al. (2004) Normal right and left ventricular mass development during early infancy. *Am J Cardiol* **93,** 797-801.
Keen EN (1955) The postnatal development of the human cardiac ventricles. *J Anat* **89,** 485-502.
Kilmer JT, Rodriguez RL (2017) Ordinary least squares regression is indicated for studies of allometry. *J Evol Biol* **30,** 4-12.
Kirkpatrick SE, Covell JW, Friedman WF (1973) A new technique for the continuous assessment of fetal and neonatal cardiac performance. *Am J Obstet Gynecol* **116,** 963-972.
Kitanaka T, Alonso JG, Gilbert RD, et al. (1989) Fetal responses to long-term hypoxemia in sheep. *Am J Physiol* **256,** R1348-R1354.
Klopfenstein HS, Rudolph AM (1978) Postnatal changes in the circulation and responses to volume loading in sheep. *Circ Res* **42,** 839-845.
Lee JC, Taylor JFN, Downing SE (1975) A comparison of ventricular weights and geometry in newborn, young, and adult mammals. *J Appl Physiol* **38,** 147-150.
Lindsey SE, Butcher JT, Yalcin HC (2014) Mechanical regulation of cardiac development. *Front Physiol* **5,** 318.
Lister G, Walter TK, Versmold HT, et al. (1979) Oxygen delivery in lambs: cardiovascular and hematologic development. *Am J Physiol* **237,** H668-H675.
Mirsky I (1974) Review of various theories for the evaluation of left ventricular wall stress. In *Cardiac Mechanics: Physiological, Clinical, and Mathematical Considerations* (eds Mirsky I, Ghista DN, Sandler H), pp. 381-409. New York: Wiley.
Mitchell G, Skinner JD (2009) An allometric analysis of the giraffe cardiovascular system. *Comp Biochem Physiol A Mol Integr Physiol* **154,** 523-529.
Moorman AFM, Christoffels VM (2003) Cardiac chamber formation: development, genes, and evolution. *Physiol Rev* **83,** 1223-1267.
Morton MJ, Pinson CW, Thornburg KL (1987) *In utero* ventilation with oxygen augments left ventricular stroke volume in lambs. *J Physiol (London)* **383,** 413-424.
Mueller CA, Seymour RS (2011) The regulation index: a new method for assessing the relationship between oxygen consumption and environmental oxygen. *Physiol Biochem Zool* **84,** 522-532.
Roche P, Czubryt MP, Wigle JT (2013) Molecular mechanisms of cardiac development. In *Cardiac Adaptations Molecular Mechanisms* (eds Ošťádal B, Dhalla NS), pp. 19-39. New York: Springer.
Rudolph AM (1970) The changes in the circulation after birth. Their importance in congenital heart disease. *Circulation* **41,** 343-359.
Rudolph AM (1985) Distribution and regulation of blood flow in the fetal and neonatal lamb. *Circ Res* **57,** 811-821.
Rudolph AM, Heymann MA (1970) Circulatory changes during growth in the fetal lamb. *Circ Res* **26,** 289-299.
Sedmera D, Ošťádal B (2012) Ontogenesis of myocardial function. In *Ontogeny and Phylogeny of the Vertebrate Heart* (eds Sedmera D, Wang T), pp. 147-175. New York: Springer.
Segar JL, Volk KA, Lipman MHB, et al. (2013) Thyroid hormone is required for growth adaptation to pressure load in the ovine fetal heart. *Exp Physiol* **98,** 722-733.
Seymour RS, Blaylock AJ (2000) The principle of Laplace and scaling of ventricular wall stress and blood pressure in mammals and birds. *Physiol Biochem Zool* **73,** 389-405.
Sirsat SKG, Sirsat TS, Faber A, et al. (2016) Development of endothermy and concomitant increases in cardiac and skeletal muscle mitochondrial respiration in the precocial Pekin duck (*Anas platyrhynchos domestica*). *J Exp Biol* **219,** 1214-1223.
Smerup M, Damkjær M, Brøndum E, et al. (2016) The thick left ventricular wall of the giraffe heart normalises wall tension, but limits stroke volume and cardiac output. *J Exp Biol* **219,** 457-463.

Smith RJ (2009) Use and misuse of the reduced major axis for line-fitting. *Am J Phys Anthropol* **140,** 476-486.
Smolich JJ (1995) Ultrastructural and functional features of the developing mammalian heart: a brief overview. *Reprod Fertil Dev* **7,** 451-461.
Smolich JJ, Walker AM, Campbell GR, et al. (1989) Left and right ventricular myocardial morphometry in fetal, neonatal, and adult sheep. *Am J Physiol* **257,** H1-H9.
Snelling EP, Taggart DA, Maloney SK, et al. (2015a) Biphasic allometry of cardiac growth in the developing kangaroo *Macropus fuliginosus*. *Physiol Biochem Zool* **88,** 216-225.
Snelling EP, Taggart DA, Maloney SK, et al. (2015b) Scaling of left ventricle cardiomyocyte ultrastructure across development in the kangaroo *Macropus fuliginosus*. *J Exp Biol* **218,** 1767-1776.
Snelling EP, Seymour RS, Green JEF, et al. (2016) A structure-function analysis of the left ventricle. *J Appl Physiol* **121,** 900-909.
Stopfkuchen H (1987) Changes of the cardiovascular system during the perinatal period. *Eur J Pediatr* **146,** 545-549.
Sylva M, van den Hoff MJB, Moorman AFM (2014) Development of the human heart. *Am J Med Genet A* **164,** 1347-1371.
Teitel DF, Iwamoto HS, Rudolph AM (1987) Effects of birth-related events on central blood flow patterns. *Pediatr Res* **22,** 557-566.
Thornburg KL, Giraud GD, Reller MD, et al. (1997) Mammalian cardiovascular development: physiology and functional reserve of the fetal heart. In *Development of Cardiovascular Systems: Molecules to Organisms* (eds Burggren WW, Keller BB), pp. 211-224. Cambridge: Cambridge University Press.
Tomanek RJ (1996) Formation of the coronary vasculature: a brief review. *Cardiovasc Res* **31,** E46-E51.
Westerhof N, Stergiopulos N, Noble MIM (2010) *Snapshots of Hemodynamics: An Aid for Clinical Research and Graduate Education, second edition, pp 45-48,* Springer, New York.
Woods Jr JR, Dandavino A, Brinkman III CR, et al. (1978) Cardiac output changes during neonatal growth. *Am J Physiol* **234,** H520-H524.
Yeager DP, Ultsch GR (1989) Physiological regulation and conformation: a BASIC program for the determination of critical points. *Physiol Zool* **62,** 888-907.
Zar JH (1998) *Biostatistical Analysis,* Prentice Hall, New Jersey.

Tables

Table 1. Scaling relationships for whole heart mass (atria + ventricles), LV mass, RV mass, and ventricular mass ratio (RV/LV), each as a function of eviscerated body mass (gastrointestinal tract removed), in fetal (N = 10) and postnatal (N = 11) Horro sheep *Ovis aries* analysed in this study.

	Fetal	Postnatal	ANCOVA comparisons of slope and (elevation)
Whole heart mass (g)	$4.90M_b^{0.88 \pm 0.26}$ $r^2 = 0.88$, $P < 0.0001$	$10.0M_b^{0.88 \pm 0.10}$ $r^2 = 0.98$, $P < 0.0001$	$F_{1,17} = 2.6\times10^{-3}$, $P = 0.96$ ($F_{1,18} = 34.6$, $P < 0.0001$)
LV mass (g)	$2.69M_b^{0.90 \pm 0.35}$ $r^2 = 0.81$, $P < 0.001$	$6.34M_b^{0.90 \pm 0.11}$ $r^2 = 0.97$, $P < 0.0001$	$F_{1,17} = 8.3\times10^{-7}$, $P = 0.99$ ($F_{1,18} = 31.2$, $P < 0.0001$)
RV mass (g)	$1.57M_b^{0.93 \pm 0.23}$ $r^2 = 0.92$, $P < 0.0001$	$2.01M_b^{0.92 \pm 0.13}$ $r^2 = 0.96$, $P < 0.0001$	$F_{1,17} = 0.028$, $P = 0.87$ ($F_{1,18} = 3.86$, $P = 0.07$)
RV : LV mass ratio	$0.58M_b^{0.04 \pm 0.30}$ $r^2 = 0.01$, $P = 0.79$	$0.32M_b^{0.02 \pm 0.15}$ $r^2 = 0.01$, $P = 0.80$	$F_{1,17} = 0.018$, $P = 0.89$ ($F_{1,18} = 17.6$, $P < 0.001$)

Equations are in the form $Y = aM_b^{b \pm 95\% CI}$, where Y is the cardiac variable of interest, a is the scaling coefficient (elevation), b is the scaling exponent (slope of the log-transformed relationship), M_b is eviscerated body mass in kg, and CI stands for confidence interval. LV is left ventricle and RV is right ventricle

Figures legends

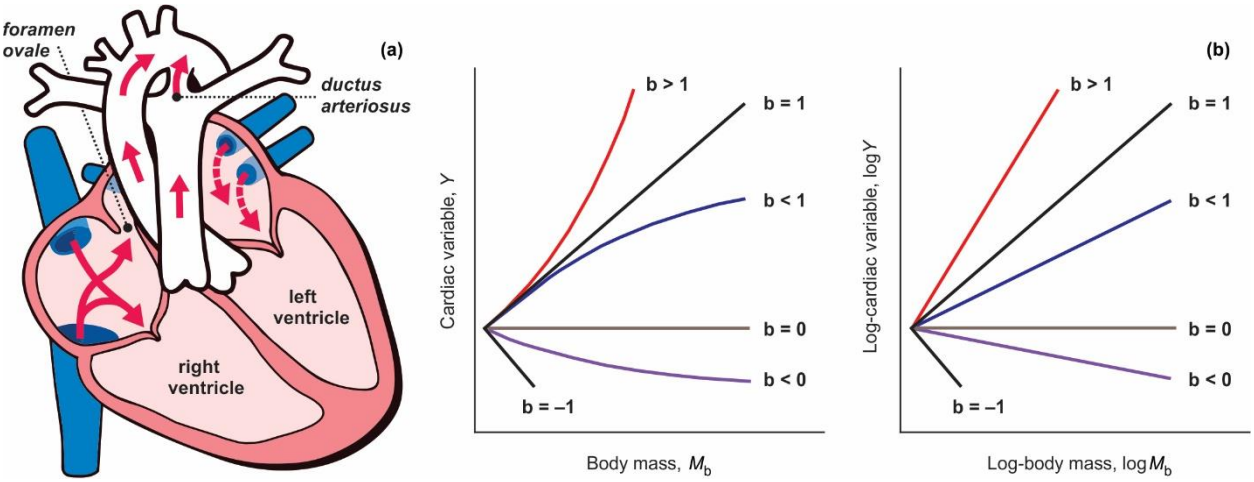

Fig 1. (a) Schematic of the fetal heart showing the *foramen ovale* communication between the left and right atria, and the *ductus arteriosus* channel between the pulmonary artery and the aorta. These shunts close soon after birth in the normal neonatal heart. (b) Scaling as a tool to assess the fetal and postnatal heart as a function of body mass across development. A cardiac variable (Y) is plotted against body mass (M_b), to produce what is often a curvilinear relationship best defined by a power equation, $Y = aM_b^{\ b}$, where a (the coefficient) represents the elevation of the curvilinear line, and b (the exponent) describes the shape of the curvilinear line. The line is straightened for statistical analysis by log transformation, and the equation becomes, $\log Y = \log a + b \log M_b$, where b retains the same value but now defines the slope of the linearized relationship. The line also can be straightened, usually for graphical purposes, by plotting the arithmetic data on logged axes.

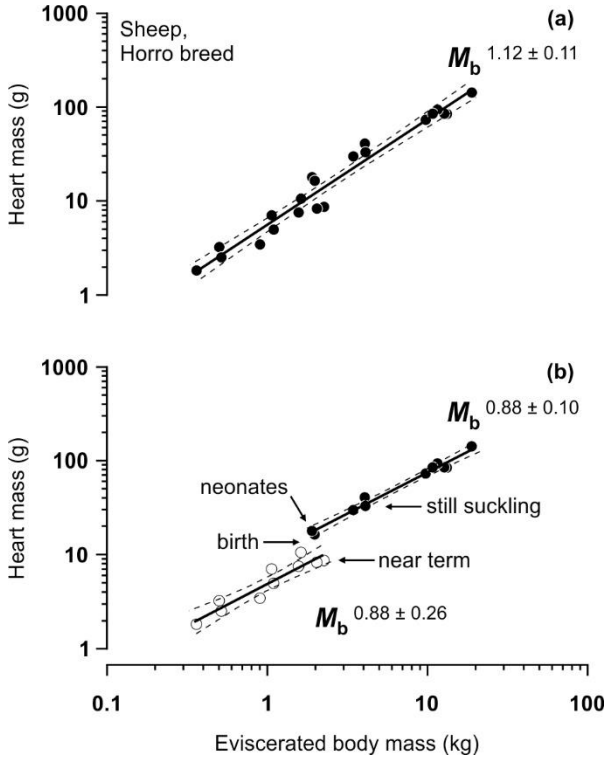

Fig 2. (a) Scaling of whole heart mass (atria + ventricles) against eviscerated body mass (gastrointestinal tract removed) across the combined fetal and postnatal development of Horro sheep *Ovis aries* analysed in this study (~50-fold body mass range; $N = 21$). (b) Scaling of whole heart mass separated into fetal (unfilled circles; $N = 10$) and postnatal life stages (filled circles; $N = 11$). Broken stick analysis confirms breakpoint at birth. The exponents (slopes) are statistically indistinguishable between fetal and postnatal groups (ANCOVA, $P > 0.05$), but the elevations are significantly different ($P < 0.05$), because heart mass doubles around the time of birth. Solid line is the regression mean, dashed lines represent the 95% confidence band. Also presented for each relationship is the scaling exponent with 95% confidence interval. See Table 1 for complete scaling relationships and statistics.

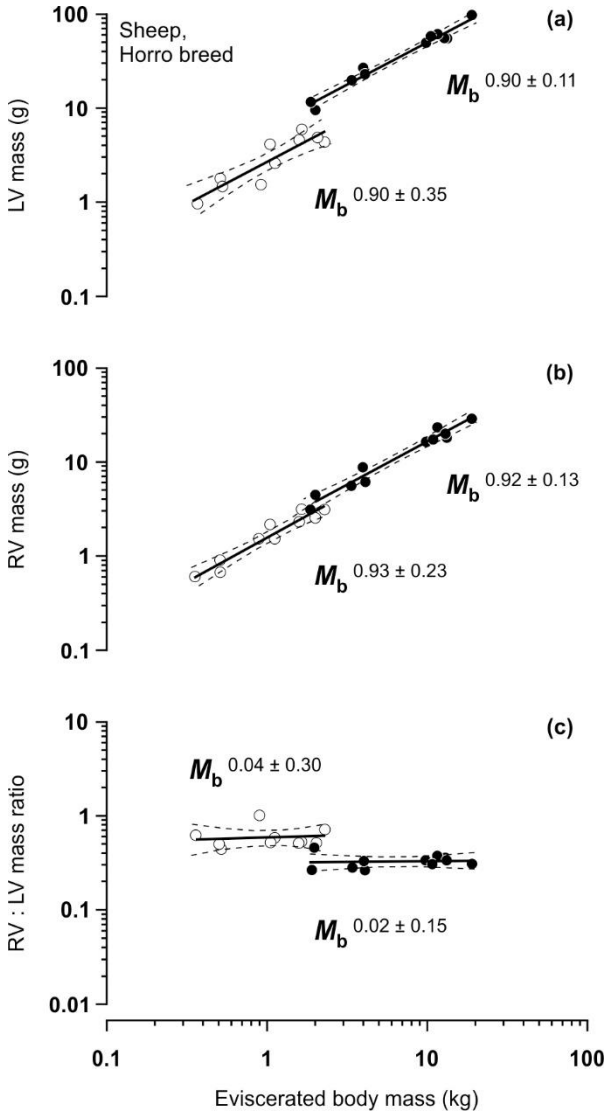

Fig 3. (a) Scaling of LV mass, (b) RV mass and (c) ventricular mass ratio (RV/LV) against eviscerated body mass in fetal (unfilled circles; N = 10) and postnatal (filled circles; N = 11) Horro sheep *Ovis aries*. Although the exponents (slopes) are statistically indistinguishable for LV mass and for RV mass when their respective fetal and postnatal groups are compared (ANCOVA, $P > 0.05$ for both LV and RV), there is a significant difference in elevation of the LV ($P < 0.05$), that is not apparent for the RV ($P > 0.05$), thus widening the ventricular mass ratio at birth. Solid line is the regression mean, dashed lines represent the 95% confidence band. Also presented for each relationship is the scaling exponent with 95% confidence interval. LV is left ventricle and RV is right ventricle.

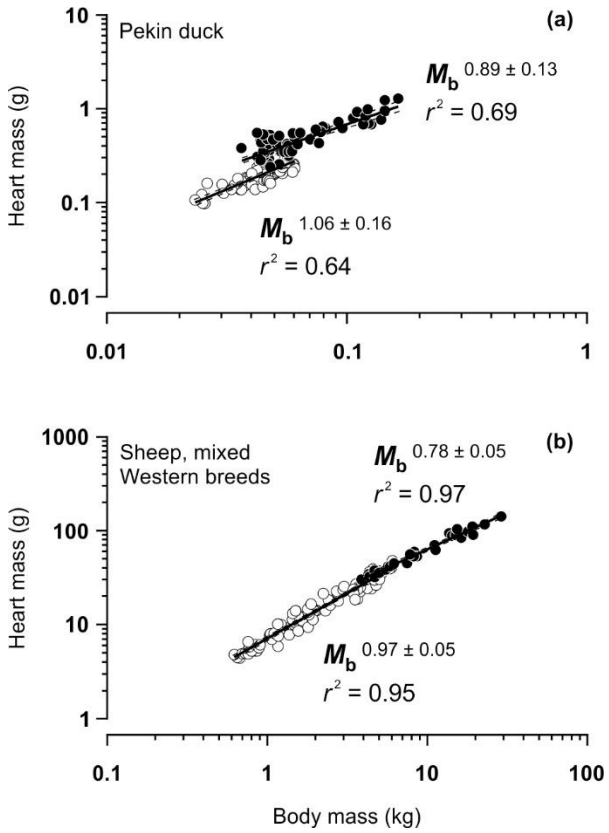

Fig 4. (a) Scaling of whole heart mass against yolk-free body mass in pre-hatch (unfilled circles; $N = 106$) and post-hatch (filled circles; $N = 92$) Pekin duck *Anas platyrhynchos domestica*, reproduced from previously published data (Sirsat et al., 2016). The exponents (slopes) are statistically indistinguishable between pre-hatch and post-hatch groups (ANCOVA, $P > 0.05$), but the elevations are significantly different ($P < 0.05$), because heart mass increases approximately 1.6-fold around the time of hatching. (b) Scaling of whole heart mass against body mass in fetal (unfilled circles; $N = 87$) and postnatal (filled circles; $N = 27$) sheep of mixed Western breeds *Ovis aries*, calculated from previously published data (Jonker et al., 2015). The exponents are significantly different between fetal and postnatal groups (ANCOVA, $P < 0.05$). Solid line is the regression mean, dashed lines represent the 95% confidence band. Also presented for each relationship is the scaling exponent with 95% confidence interval and the coefficient of determination.